| REPORT DOCUMENTATION PAGE | Form Approved OMB No. 0704-0188 |
|---|---|



| 1. REPORT DATE *(DD-MM-YYYY)* | 2. REPORT TYPE | 3. DATES COVERED *(From - To)* |
|---|---|---|
| 30/01/2007 | Final | Jan 2001--Oct 2006 |

**4. TITLE AND SUBTITLE**

Continued development of the Look-Up-Table methodology for interpretation of remotely sensed ocean color

**5a. CONTRACT NUMBER**

**5b. GRANT NUMBER**

N00014-01-1-0201

**5c. PROGRAM ELEMENT NUMBER**

**6. AUTHOR(S)**

W. Paul Bissett

**5d. PROJECT NUMBER**

**5e. TASK NUMBER**

**5f. WORK UNIT NUMBER**

**7. PERFORMING ORGANIZATION NAME(S) AND ADDRESS(ES)**

Florida Environmental Research Institute
10500 University Center Drive, Suite 140
Tampa, Florida 33612

**8. PERFORMING ORGANIZATION REPORT NUMBER**

**9. SPONSORING/MONITORING AGENCY NAME(S) AND ADDRESS(ES)**

Office of Naval Research
875 North Randolph street
Arlington, VA 22203-1995

**10. SPONSOR/MONITOR'S ACRONYM(S)**

ONR

**11. SPONSOR/MONITOR'S REPORT NUMBER(S)**

**12. DISTRIBUTION/AVAILABILITY STATEMENT**

Approved for Public Release; Distribution is Unlimited

**13. SUPPLEMENTARY NOTES**

N/A

**14. ABSTRACT**

See Attached

**15. SUBJECT TERMS**

Remote sensing, colored dissolved organic matter, CDOM, inherent optical properties, IOPs, bathymetry, HyperSpectral Imaging, HSI, Look-Up-Table, LUT

| 16. SECURITY CLASSIFICATION OF: | | | 17. LIMITATION OF ABSTRACT | 18. NUMBER OF PAGES | 19a. NAME OF RESPONSIBLE PERSON |
|---|---|---|---|---|---|
| a. REPORT | b. ABSTRACT | c. THIS PAGE | | 2 | Beverly Walters |
| | | | | | 19b. TELEPHONE NUMBER *(Include area code)* 813-866-3374, ext. 101 |

**ABSTRACT**

The LUT approach to inverting ocean color spectral remote sensing data seeks to use the greater number of degrees of freedom available in the hyperspectral data to retrieve (1) bathymetry, (2) water column IOPs, and (3) bottom identification in optically-shallow waters. We have discovered several significant findings in developing this approach. First is that the quality of the input measured spectra is critical to the success of the technique. Thus, the characterization and calibration of the measurement sensors, as well as the accurate characterization of any environmental noise (e.g. atmospheric correction) is critical for success. Second, the best approach to this type of inversion is to use hybrid matching techniques that focus on total magnitude of the measured signal, as well as spectral angle. Third, when perfection in calibration or removal of environmental noise is unattainable, the best approach uses a knowledge-based technique to refining the LUT search. For example, in waters deeper than 2 meters, it may be useful to exempt wavelengths longer than 600 nm from the database search criteria so that residual skylight reflectance that has not been removed from the sensor measured radiance does not reduce the accuracy of the LUT retrievals.

# Continued Development of the Look-Up-Table Methodology for Interpretation of Remotely Sensed Ocean Color

W. Paul Bissett
Florida Environmental Research Institute
10500 University Center Drive
Suite 140
Tampa, FL 33612

Award Number: N00014-01-1-0201

phone: (813) 866-3374 x102 fax: (813) 977-8057 email: pbissett@feriweb.org

http://www.feriweb.org

## LONG-TERM GOALS

Remote sensing algorithms for the marine environment have traditionally relied upon semi-empirical approaches to determining water column properties. These algorithms are usually depth-integrals of a proxy of desired information, i.e., chlorophyll algorithms are a proxy for water column autotrophic biomass. The goal of this work is to use the increased spectral resolution of current satellite and aircraft data systems to solve for the depth-dependent optical properties of interest, e.g., absorption and scattering, as well as the depth-dependent distribution of the individual optical constituents, e.g., diatoms, dinoflagellates, cyanobacteria, CDOM, and sediment. This will be accomplished by creating a large dataset of simulated remote sensing reflectance, $R_{rs}$, using a radiative transfer model and developing a look-up-table approach to $R_{rs}$ inversion.

## OBJECTIVES

1) Help develop the code to quickly run $>10^7$ calculations of $R_{rs}$.

2) Provide IOPs for individual optical constituents and establish their depth-dependent profiles for simulations.

3) Help develop search optimization schemes to invert satellite and aircraft $R_{rs}$ to depth-dependent optical properties and constituent profiles.

## APPROACH

Various ocean color remote sensing instruments are now available or under development. These sensors all measure spectral upwelling radiances which, after atmospheric correction, give the spectral water-leaving radiance $L_w(\lambda)$ or an equivalent remote-sensing reflectance $R_{rs}(\lambda)$; here $\lambda$ is the wavelength. The end goal of ocean color remote sensing is to extract from $L_w$ or $R_{rs}$ useful environmental information such as the absorption and scattering properties of seawater constituents (phytoplankton, dissolved substances, mineral particles, etc), chlorophyll concentration, or bottom bathymetry and bottom type in shallow waters. Currently available algorithms for extracting environmental information generally use empirically derived correlations between the quantity of

interest and the ratio of $L_w$ or $R_{rs}$ at two wavelengths. For example, the algorithm for extracting chlorophyll concentrations from SeaWiFS data is based on the ratio $R_{rs}(490\ nm)/R_{rs}(555\ nm)$ (O'Reilly et al., 1998). Such ratio algorithms do not make full use of the available spectral data even in the SeaWiFS sensor, nor can they be expected to provide much information about water composition (as opposed to just total absorption or total chlorophyll concentration). Ratio algorithms provide erroneous results if applied to waters outside the range of the empirical data from which they were derived. For example, the OC2 chlorophyll algorithm, which was derived for Case 1 waters, will provide incorrect chlorophyll values if applied to Case 2 waters containing mineral particles or high levels of CDOM (Colored Dissolved Organic Matter).

The Hydrolight radiative transfer numerical model (Mobley, 1994) gives an exact solution of the in-water radiative transfer equation given the water inherent optical properties (IOPs, namely the absorption and scattering properties of the water body), the incident sky radiance, and the bottom depth and reflectance (bottom BRDF). The water IOPs can be built up from any number of components, such as various microbes, dissolved substances, organic detritus, mineral particles, or microbubbles. For remote-sensing purposes, the relevant Hydrolight output is the spectral water-leaving radiance. We will first construct a database containing a large number of Hydrolight runs corresponding to different combinations of water composition (different microbial, dissolved, or mineral substances at different concentrations), sky conditions (different solar angles and atmospheric conditions), sensor viewing directions, wavelengths, and so on. The resulting water-leaving radiances in the database, $L_{wd}$, are in principle all different. Given a measured water-leaving radiance $L_{wm}$ (obtained from atmospheric correction of an at-sensor radiance), one can then "look up" the $L_{wd}$ spectrum that most closely matches $L_{wm}$. The water IOPs and bottom conditions in the actual water body are then taken to be the values that were used in Hydrolight to generate the selected $L_{wd}$. We thus effect an inversion of the measured spectral signature by the conceptually simple process of spectrum matching and then looking up the answer in the database.

The work is part of a larger project led by C. Mobley of Sequoia Scientific, Inc. (N0001400D01610001)

**WORK COMPLETED – 2001**

The HYDROLIGHT v4.1 software package that contains the numerical solution to the RTE using invariant imbedding techniques includes over 60 Fortran program units, as well as a supplementary Graphical User Interface, IOP sub-models, and supplementary data files. The implementation of this software over large spatial and temporal domains is cumbersome within a reasonable amount of time. Thus, the core of the numerical invariant imbedding solution has been re-written and condensed into a single Fortran 90 subroutine (excluding 3 subroutines containing general mathematical algorithms that are freely available from the NETLIB library). Input variables to the subroutine are the depth-dependent total absorption, particulate scattering, and scatter phase function, as well as the total geometric depth, solar zenith angle, cloud fraction, and spectral incident downwelling direct and diffuse irradiances. Output are data files containing the surface emergent polar flux ($L_w$), the specularly reflected radiance at the surface, and the in- water irradiance fields (upwelling/downwelling, scalar/planar) at 1.0 meter increments from just beneath the surface to the bottom.

The quadrature discretization technique as described by (Mobley, 1994) is maintained at 20 theta (polar) quads and 24 phi (azimuthal) quads, yielding a 10 degree angular resolution in the polar and 15 degree resolution in the azimuth. Reducing this resolution can increase the computational speed.

However, for this first step we maintain the full quad resolution so that no information regarding the angular distribution of the light field immediately above and below the air/sea interface is "smeared out". This is particularly crucial when considering the interaction between the solar zenith and azimuth angles and the local sea surface realized transmittance and reflectance functions, as they become less accurate with decreased quad resolution.

A large increase in computational efficiency was achieved by only solving the invariant imbedding solution to the RTE for the first mode of the Fourier polynomial analysis. Briefly, the HYDROLIGHT 4.1 RTE solution radiance amplitudes in each quad have a Fourier polynomial with 12 modes. Each upward integration of the Riccati differential equations that solve for the standard operators (transmittances and reflectances) of the radiance amplitudes must be repeated 13 times for both the sine and cosine modes of the Fourier polynomial, resulting in a total of 26 integrations in the upward sweep for a single depth of interest. Unfortunately, for a complete solution to radiances in all quads there can be no truncation of this series. Fortunately, to solve only for irradiances as well as the radiance values of the "polar caps" only the first Fourier component, $l = 0$, need be considered. Since all sine mode amplitudes are zero for $l = 0$, we reduce 26 integrations of the "upward sweep" to only one. This is possible because the first Fourier component of the radiance amplitude has no azimuthal dependence, and so quantities that also have little azimuthal dependence – irradiances and polar radiance – can be computed only from the first Fourier component. It is important to emphasize here that the full azimuthal quad resolution was maintained (n=24) only to address the complexities of the air/sea interface. This is because "when the upper boundary is involved, the amplitude for one *l*-mode is directly coupled to the amplitudes for all other *l*-modes" (Mobley, 1994). Accordingly, we describe the reflectance and transmittance of radiance through the air/sea interface for all quads and *l* - modes. Once through the air/sea interface, however, the *l*-modes are de-coupled, allowing us to ignore the remaining *l*-modes when integrating the Riccati differential equations at depths of interest.

**RESULTS -2001**

Given the same depth dependent IOP's, surface boundary condition, bottom boundary condition (reflectance), and using the same discretized phase function for particle scattering, our results from OPTIMv1 match those of HYDROLIGHT v4.1 quite well, as shown in Figure 1. These validation runs were for a depth of 20 meters, output at every meter, and a spectral resolution of 5 nm from 400 to 700 nm, yielding 60 wavebands. Results from all depths and wavebands are shown in Figure 1. Examination of Figure 1 reveals that there is a very slight underestimation of $L_w$ and $E_u$ by OPTIMv1 when compared to HL. This may be due to the scattering of radiance from lower quads into the polar cap that is accounted for only by the full HL solution. The computational reduction between the full HL solution and OPTIMv1 can be seen in Figure 2. Greater computation reductions may be possible through any reduction in depth resolution, spectral resolution, and quad resolution. However, we currently prefer to maintain this resolution for comparisons to other programs. At an average computation time of one waveband every two seconds this data base can grow to over 15 million $R_{rs}$ values in a year's time using a single Intel PIII processor. We expect significant decreases in processor computational time when the code is transported to the NRL Origin 3800. In addition, the Origin 3800 is a massively parallel machine that will also greatly reduce the wall clock computation time through simultaneous calculations on >100 processors.

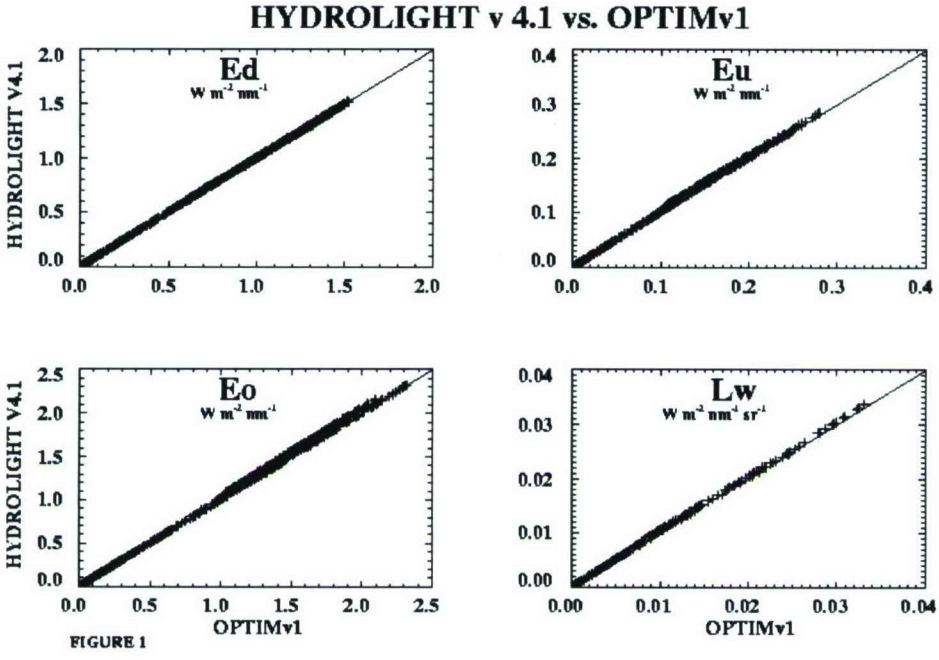


*Figure 1. Comparison of Hydrolight 4.1 and OPTIM 1 results for the same IOP data set and downwelling irradiance field.*

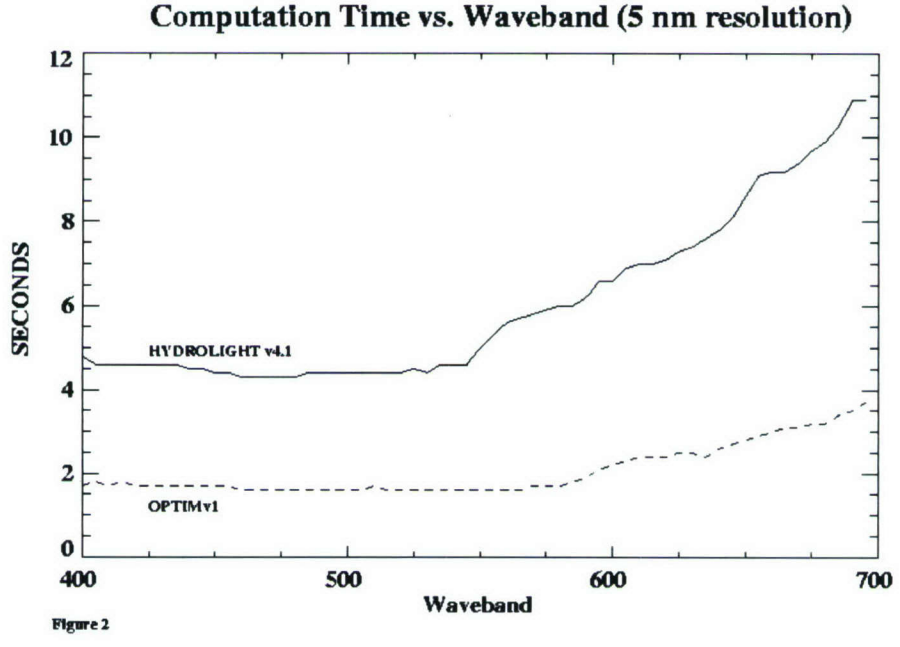


*Figure 2. Reduction in computational speed for OPTIMv1 versus Hydrolight 4.1.*

## WORK COMPLETED - 2002

This year's work consisted primarily of algorithm development and evaluation using Hydrolight-generated synthetic data. Representative IOPs and bottom reflectances measured during the CoBOP field experiments at Lee Stocking Island (LSI), Bahamas were assembled. Figure 3 shows some of the bottom reflectance spectra obtained in the vicinity of LSI. These data, along with measured and modeled IOPs for Case 1 and 2 water and bottom reflectances from other locations, were used in a special version of Hydrolight to generate a database of 2,200 $R_{rs}$ spectra. An independent test set of $R_{rs}$ spectra was similarly generated. These initial spectra were used for debugging code, examining ideas and spectrum-matching algorithms, and discussion of database formats, before proceeding with the generation of a larger database for operational use.

Six different spectrum matching algorithms were developed and compared using the pseudodata (for which the "correct answer" is known). The initial results were very encouraging. We therefore then generated an expanded database of 5,750 $R_{rs}$ spectra for use in processing a PHILLS image acquired on May 20, 2000 during the closure experiment of the final CoBOP field year. These spectra were generated by 5,750 independent Hydrolight runs using all combinations of 10 sets of water inherent optical properties, the 23 bottom reflectance spectra of Figure 3, and 25 water depths. These $R_{rs}$ spectra are shown in Figure 4. These spectra are now being used for pixel-by-pixel processing of the PHILLS image.

This work does not involve the acquisition of field data. Therefore, no data have been submitted to any national data archive.

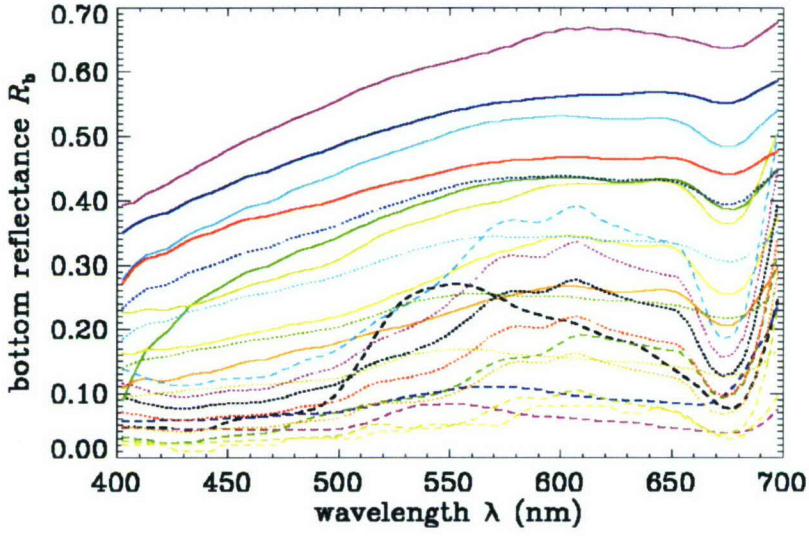


***Figure 3. The 23 bottom reflectance spectra used to generate the remote-sensing reflectance database of Figure 2. Solid lines are measured reflectances for sediments (ooid sand, grapestone, etc). The dashed lines are measured spectra for biota (seagrass, corals, red and green algae). The dotted lines are spectra for combinations (e.g., 40% sea grass and 60% sand).***

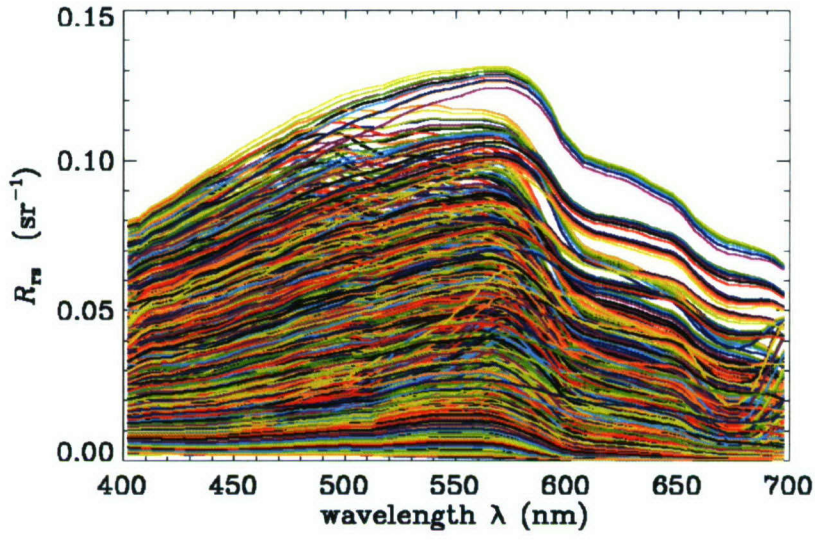


***Figure 4. The 5,750 remote-sensing reflectance spectra (10 sets of IOPs x 23 bottom reflectances x 25 bottom depths) being used to match PHILLS spectra pixel by pixel.***

**RESULTS - 2002**

The algorithm evaluation based on the pseudodata led to the following conclusions. Details can be found in (Mobley et al., 2002).

- The database search problem is numerically simpler and faster than originally thought. For example, doing a brute-force search of 100,000 randomly generated 60-wavelength $R_{rs}$ spectra to see which one is closest to a given spectrum requires only 0.1 seconds on a 600 MHZ PC. In practice, spectral databases will likely contain far fewer spectra, and search times will not be a problem. This means that near-real-time processing of PHILLS images may be feasible.

- The choice of spectrum-matching algorithm may not be critical, and wavelength-uncorrelated random noise is not likely to be a problem. The six different spectrum-matching algorithms evaluated so far performed comparably in finding the closest database spectrum. There are some minor differences, but all did rather well at extracting environmental information when applied to the test spectra. Wavelength-uncorrelated random noise does not greatly impede the spectrum matching. (However, it remains to be seen if there are significant differences in algorithm performance when applied to real data, which may have noise characteristics that favor particular search algorithms.)

- Finally, the LUT approach to retrieving IOP, bottom reflectance, and bottom depth information from remote-sensing reflectances performed well with the test data.

The details of this work will be reported at the Ocean Optics XVI conference.

## WORK COMPLETED - 2003

The optical complexity of the near shore coastal environment has been a challenging area for traditional passive remote sensing systems to accurately classify. Recent advances in passive HyperSpectral Imaging (HSI) have shown it to be a valuable tool in the characterization of these areas. However, the HSI algorithms to map this environment require the simultaneous resolution of water type, bottom type, and depth. While these methods have produced admirable results (Kohler, 2001; Lee et al., 1999; Lyzenga, 1978; Philpot, 1989), better constraining these equations should greatly improve the accuracy of the outcome. Bathymetric LIDAR systems have been demonstrated to reliably produce very accurate estimates of water depth (Guenther, 2001). Thus, the coupling of the two systems should at a minimum produce improved maps of in-water and bottom optical properties by better constraining the passive remote sensing mapping models. In the fall of 2002, the PHILLS2 passive hyperspectral sensor and the SHOALS bathymetric LIDAR were deployed over Looe Key, Florida. While the sensors were flown independently, the data was collected nearly simultaneous to illustrate the merits of a coupled system, as well as provided ground truth data for the HSI/LUT development.

The LUT technique (see Mobley Progress Report, N0001400D01610001 for details of the LUT development) was applied to the atmospherically corrected HSI data (see Bissett Progress Report, N000140010514, and Kohler Progress Report, N000140310626, for details of atmospheric correction). The LUT results return estimates of water column IOPs, bathymetry, and bottom classification. Comparisons to the bathymetric LIDAR were completed and errors were analyzed. HSI flight data and metadata may be found at http://www.flenvironmental.org/Projectpages/flightlogindex.htm.

## RESULTS - 2003

Light is attenuated exponentially in water at spectrally different rates. In shallow waters where the bottom can be distinguished with remote sensing techniques, the determination of water depth is critical to retrieving the vertical structure of IOPs, as well as bottom classification. Any remote sensing algorithm that seeks to retrieve these littoral zone properties will have to simultaneously solve for bathymetry. The HSI/LIDAR data set provides a unique opportunity to test an algorithm approach over a statistically significant number of points from an IHO level 1 bathymetric system to provide 1) robust validation, and 2) error analysis. Figure 5 shows an RGB of the atmospherically corrected HSI data from Looe Key. Figure 7 shows the HSI bathymetry estimates. Figure 7 is the RGB with an overlay of ~$1.3 \times 10^6$ collected LIDAR soundings used for the initial comparisons.

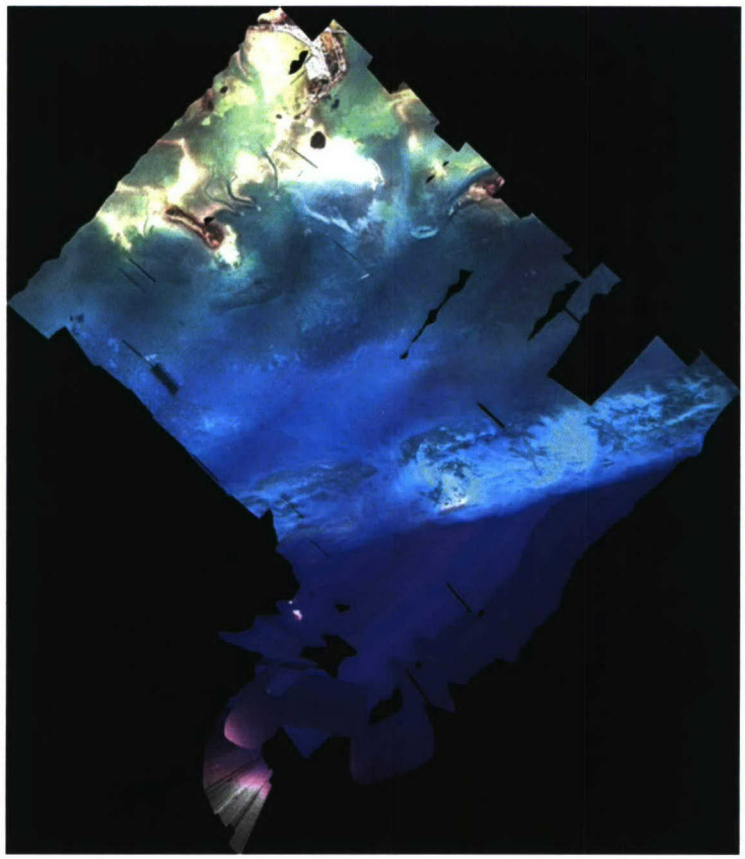

***Figure 5. False color composite of the data HSI collected at Looe Key, FL during October, 2002. The area at the bottom is not part of the analysed data as it was collected during aircraft maneuvers resulting in direct sun reflection into the sensor.***

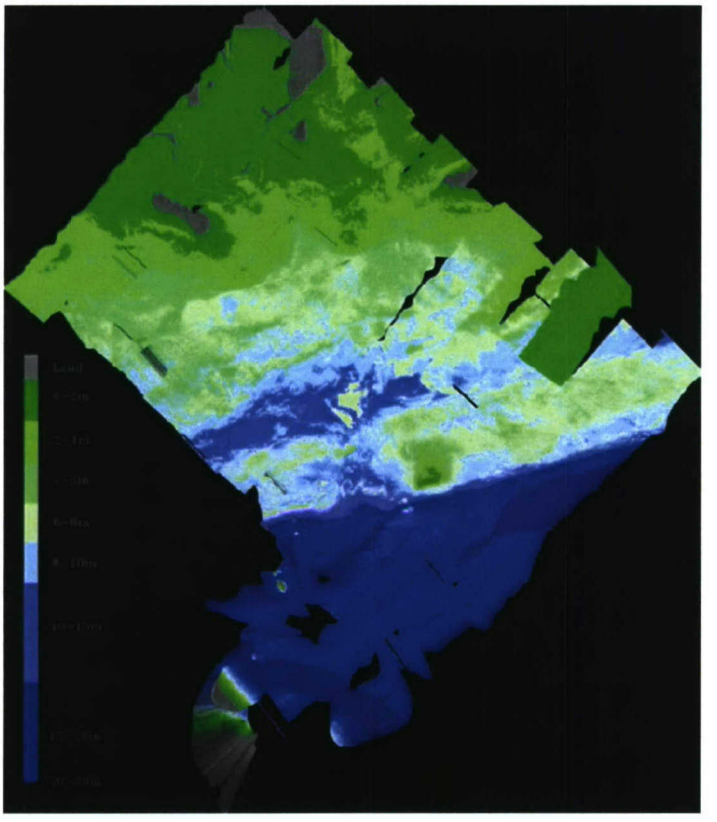

***Figure 6. LUT estimated bathymetry for Looe Key, FL using HSI data shown in Figure 1. Color contours are in 2 m intervals from dark green to dark blue, as shown by scale on left of image.***

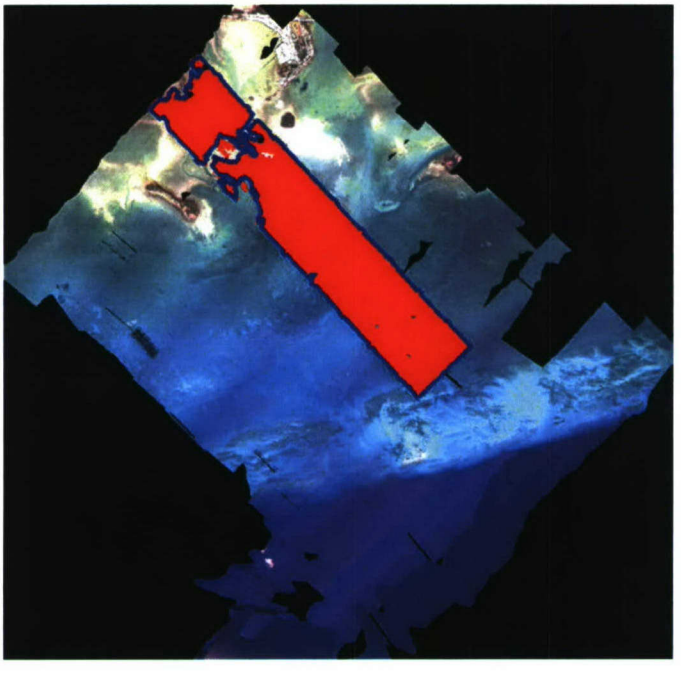

***Figure 7. SHOALS bathymetric LIDAR coverage for data analysis. Approx. 1.3 million sounding in the area marked in red.***

These bathymetric results from the LUT retrieval suggest that the approach is not only reasonable, but statistically significant, particularly in regions where the bottom spectra and classification are well described. Figure 8 shows an enhanced version of the error analysis, highlighted the region of maximum errors, outside of the expected Gaussian distribution if the errors were randomly distributed around zero. The highlighted region of the graph is a substantial underestimation of the bottom depth by the HSI/LUT technique. These errors are from the Hawk Channel region (seen in Figure 5 and 7 as a slightly darker water mass) and seem to be a function of an inaccurate bottom spectra or IOP set in the LUT database.

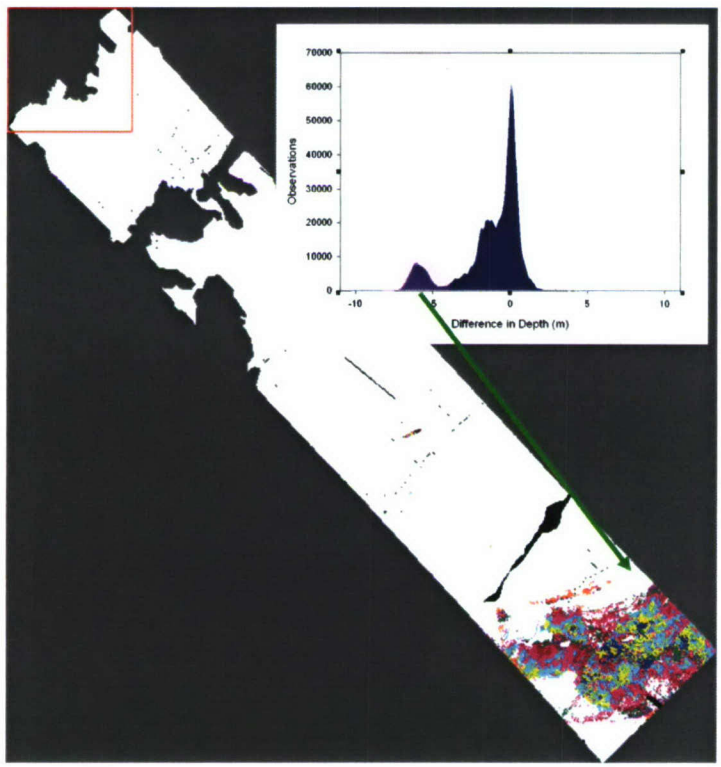


***Figure 8. Error analysis of the HSI/LUT estimated bathymetry. The data spanning from the upper left to the lower right of the figure is the sounding overlay seen in Figure 3. The colors highlight the area of maximum error between the HSI/LUT estimated bathymetry and the SHOALS LIDAR bathymetry. The inset figure is the distribution of errors over the combined dataset, (LUT-LIDAR), where the majority of points are centered at zero. The large deviations from the expected Gaussian distribution of errors are highlighted in the inset and correspond to the colored region in the image. The other region outside of the Gaussian curve (at ~-1.5 m) appears to correspond to mechanical errors in the SHOALS system.***

There is another small region centered around -1.5 meters in error which appears to be the function of mechanical errors in the SHOALS system which caused demonstrated stripping in the bathymetric soundings (data not shown). Outside of these regions, the errors appear to be randomly distributed at zero. Over the whole dataset, 56% of the LUT estimates are $\pm 1$ m, and 76% are $\pm 2$ m, suggesting that this methodology is a valid approach to retrieving bathymetry, water column IOPs, and bottom classification from hyperspectral imagery.

**WORK COMPLETED - 2004**

In addition to the work described by the lead PI C. D. Mobley (N0001400D01610001), we performed additional numerical experiments that should be mentioned in the joint progress report. It became clear in some of our early work that there were some sensitivity studies which needed to be accomplished to optimize the LUT database for the sensor providing the spectral information. Bathymetric sensitivity revolves around the number and size of the depth spacing in the LUT database. If our depth resolution is too coarse, we loose accuracy by forcing bathymetric errors into IOP and/or bottom reflectance errors. If the depth resolution is too fine, we waste resources in generating a LUT with more depths then needed, and correspondingly, the matching process is slower as it increases the number of entries to search. Lastly, having finer depths than required may also give misleading accuracy estimates to the user.

A generalized version of the problem is, having a depth $d_1$ in LUT, we want to find a depth $d_2$, such that $d_2$ is as close to $d_1$ as possible and also that the hyperspectral signals for both the depths are different enough for a search algorithm to potentially be able to distinguish between them. The derived depths should be for a generic sensor and conditions, so that it is applicable to all the sensors. The approach taken was to generate a LUT with depth increments of 1 cm up to 50 meters for an environment with pure water and clear sand. Having this LUT, we then try to extract adjacent depths that have enough difference in signal for a search algorithm to potentially distinguish between them. As pure water and clear sand makes the most ideal scenario for determining bathymetry, depths derived for such a scenario will be a comprehensive list usable for any real life environment. This led to the creation of a LUT with 5000 depths from 1 cm to 50 m for pure water and clear sand.

The determination of "enough" difference in signal is sensor dependent. Different sensors have dynamic range and signal to noise (SNR) potentials that may affect the number of depths resolvable to generate bathymetry estimates. A $n$ bit sensor can output $2^n$ discrete values (dynamic range). We estimated (not shown here) that the combination of sensor soft saturation, atmosphere, and water effects for any sensor would reduce the dynamic range of shallow water pixels by 24% of the total $2^n$ discrete values. To distinguish between any two depths, the signal value of at least one band in the signal should be different.

This approach must include an estimate of SNR, so as not to over-estimate the ability to resolve bathymetric differences. A signal to noise ratio (SNR) of 200 for remote sensing reflectance is used for this study. This is several factors higher than the SNR for remote sensing reflectance from any sensor currently available today (note, this is not radiance at the sensor SNR, but remote sensing reflectance SNR which includes the removal of the atmosphere). As the brightest water signal will be $(0.24)\ 2^n$, at a SNR of 200 the minimum detectable signal may be estimated as $(0.005)\ (0.24)\ 2^n = (0.0012)\ 2^n$. Thus, if any one of the signal bands of any given adjacent depths is different by the computed digital SNR for that sensor, an algorithm may potentially distinguish between them.

**RESULTS - 2004**

As noted above, we generated a LUT with 5000 depths, starting from 1 cm up to 50 meters with 1 cm spacing. The LUT was then normalized and each signal value was converted to a discrete value. The brightest signal in the LUT was give the value of $(0.24)\ 2^n$. The rest of the LUT signals were then scaled using their ratios to the brightest signal. Starting from the first depth entry in LUT, at 1 cm, the nearest depth from it, which had at least one band in the spectrum different by the computed digital SNR was found and added to the list of required depths. This added depth then became the reference

and the nearest distinguishable depth from this point was then found. Using this method for a 14 bit sensor, 292 depths were found that matched the criteria.

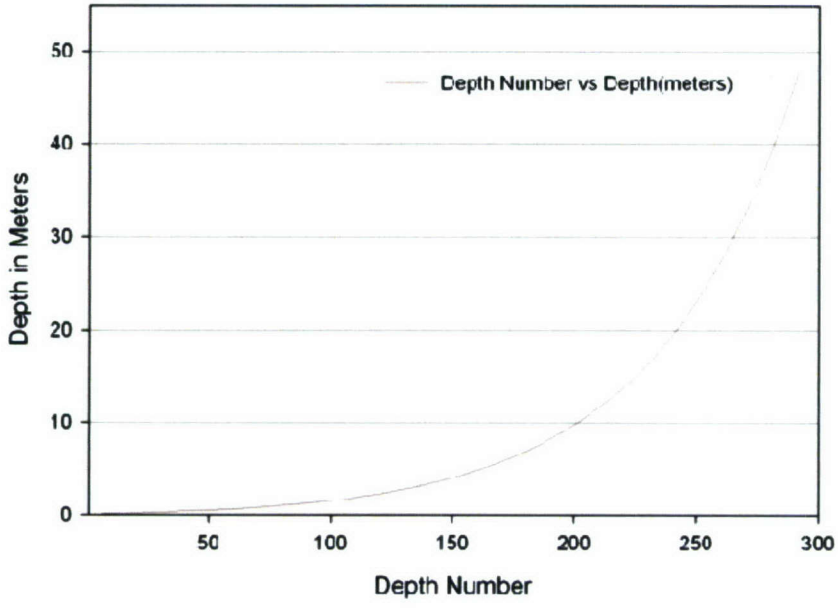


***Figure 9. Graph plotting actual depth (y axis) versus depth bin number (x axis) for a 14 bit sensor yielding a 200:1 SNR water-leaving radiance spectra. This graph shows that the resolving power of the spectral signal decreasing nearly exponential with depth, such that the most resolution in bathymetry is in the shallower depths.***

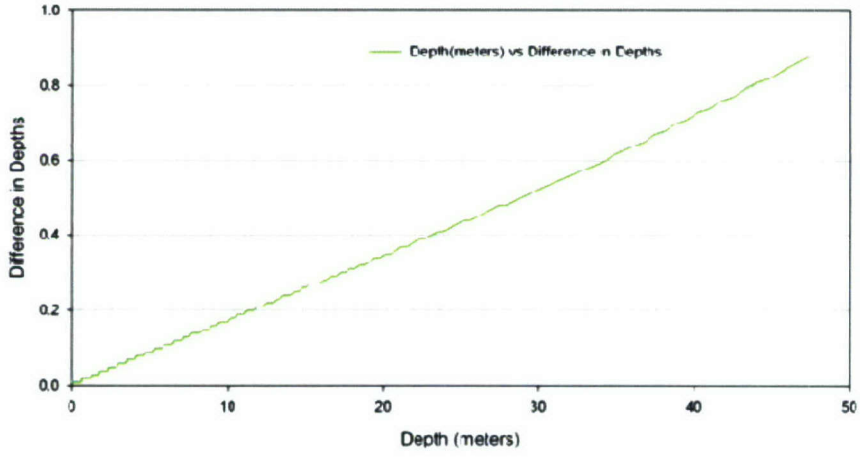


***Figure 10. Graph plotting depth with difference between adjacent resolvable depths. In this case, the graph shows that the deeper the bathymetry, the greater the difference between adjacent depth levels, which are resolvable with a 14 bit, 200:1 SNR spectral sensor.***

As shown in Figure 9 and Figure 10, as depth increases, the difference between adjacent depths also increases. With the increase in the depth, the difference between any two spectral signals observed weakens, and it becomes increasingly difficult to distinguish between two adjacent depths.

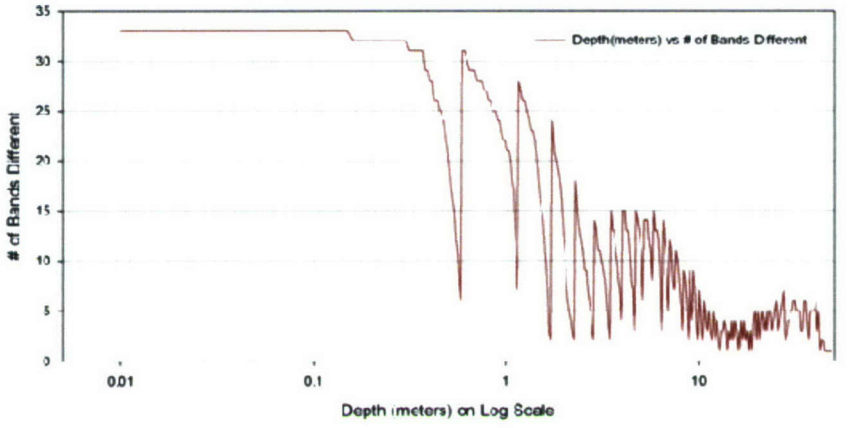


***Figure 11. Graph plotting the number of bands which are significantly different, defined by the bit resolution of the sensor and the sensor SNR (in this case 14 bit, 200:1 SNR), between adjacent depth bins. In the shallowest depths, the vertical resolution was 1 cm, however, by 0.5 m it becomes very difficult to distinguish any two depths, i.e. 0.50 and 0.51 m, by a 1 cm difference. At this point, the vertical resolution between two depths jumps to 2 cm, and the number of bands which are difference commensurately jumps. This process continues to the deepest depths, where the minimum vertical resolution that may be distinguish in nearly 1 m (Figure 10).***

As observed in Figure 11, the difference between the signals of adjacent depths reduces as the depth increases. The deeper the bathymetry for any given depth increment, the smaller the number of bands that are significantly different. At some point, two depth intervals are nearly indistinguishable. This gives rise to an increase in the depth increment, which in turn results in a sharp increase in the number of different bands.

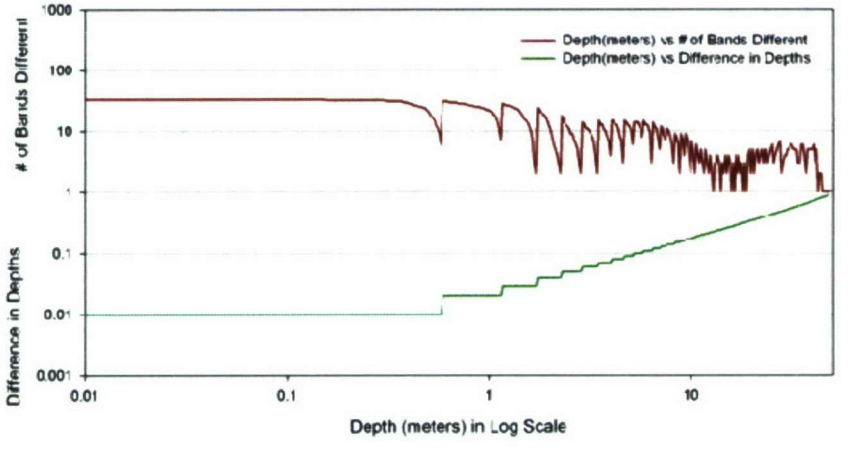


***Figure 12. Difference between adjacent depths and number of bands different plotted as a function of depth. Figure 11 is included at the top of the figure (in log space) to demonstrate the increase in depth increment that corresponds to the jump in resolvable bands within the spectra.***

Figure 12 confirms that whenever the discretization in depths increases, correspondingly there is a jump in the number of bands that are different.

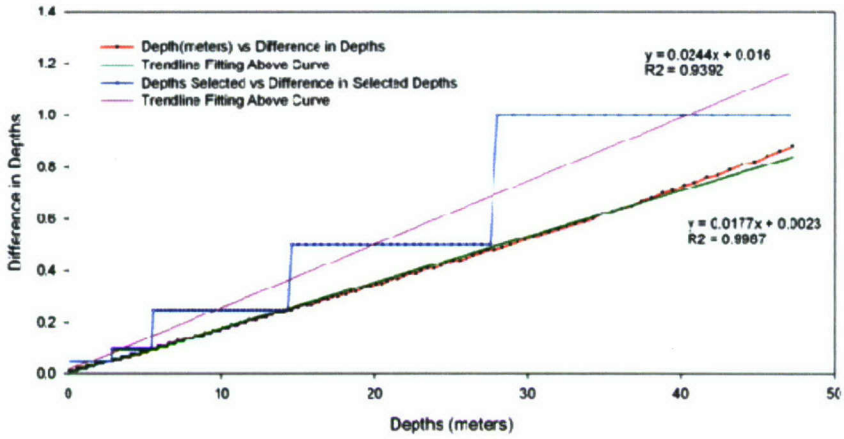


***Figure 13. The selected depth discretizations for the 14 bit, 200:1 SNR idealized sensor (blue line). Red line is the continuous difference demonstrated in figure 11 and 12. The green line is the trend line that best fits the continuous data, and the purple line is the trend line that best fits the selected discretization.***

The red line in Figure 13 plots the difference in depths for all the depths selected. Any depth discretization that falls below this line is too fine for that particular sensor to distinguish. Although, ideally we want all the depths selected to be on this line, it is practically not feasible to do so. Even though the sensor can resolve depths starting from 1 cm, it might not be needed for a particular application to have such fine depth discretization. For our application we chose to start from 5 cm. Also, by following that trend line, we might get depths that generate a false sense of accuracy. For example, the selected depths might have a depth of 39.74 meters and the next depth of 40.12 meters. If we report a depth of 40.12 meters for a particular point, it might induce the user to believe that we are able to resolve depths with a 1 cm accuracy even at 40 meters which is certainly not true. Thus rather than having a continuous discretization, a fixed discretization is chosen, which corresponds to the resolution of the sensor and the general application of the LUT methodology. For our application we choose depths discretization of 5 cm, 10 cm, 25 cm, 50 cm, and 1 meter.

## WORK COMPLETED - 2005

In addition to the work described by the lead PI C. D. Mobley (N0001400D01610001), we performed other code development and numerical experiments that should be mentioned in the joint progress report.

The expansion of the LUT database to >200,000 entries increased the processing time of the Looe Key image from hours to weeks. Any further development of the LUT techniques require us to recode the spectrum matching code to more finely select appropriate spectrums to test against the measured $R_{rs}$ spectra. This included better memory management, spectra magnitude threshold test, and more streamlined looping and table searching.

Once the streamlining was complete, we were able to begin bathymetric error analysis of the 12K vs. 200K LUT. The results were far different than expected and has forced us to address sensor and environmental noise (see Bissett N00014-04-1-0297) within the context of developing a more complete LUT approach.

**RESULTS - 2005**

The previous LUT table entries (11,000 total combinations of bathymetry, bottom type, and water column IOPs) were expanded to a total of 235,625 entries. In addition to the new bottom types and waters added to the LUT, the depth discretization was made finer. A detailed analysis of the sensor was done to find the discretization that was optimal for the current sensor and the applications; and it resulted in 145 optically unique depths (http://www.feriweb.org/Publications_ppts/2004_FERI_0003_U_D_LUT_Sen.pdf). As the LUT was made more diverse with added waters, bottoms, and a finer depth discretization, the inherent thought was that it will enhance the classification accuracy and that the derived bathymetry using the new LUT will have less average error per pixel then previous LUT did. To evaluate this, the Looe Key image, which had an average absolute error of 1.80 m in the depth derived with the old LUT as compared to SHOALS data, was classified using the new LUT.

Although, it was known that the time taken to classify the image would not be linear with the growth in the entries of LUT, the time taken to classify using the new LUT was operationally infeasible. At the rate that it was executing, it would have had taken about 15 days to classify just that one image. Thus, efforts were made to optimize the code for faster execution time. Bottlenecks that were responsible for slow execution were found in the code and were replaced with modified faster code. The resultant code took 6 hours to classify the image.

Contrary to the improvements expected using the new LUT, the derived bathymetry had a far worse average absolute error of 3.0 m. Some areas of the image had very low classification accuracy. The bathymetry derived from the new LUT in those areas were consistently less than the depth derived from SHOALS on an order of 8 to 10 meters (Figure 14).

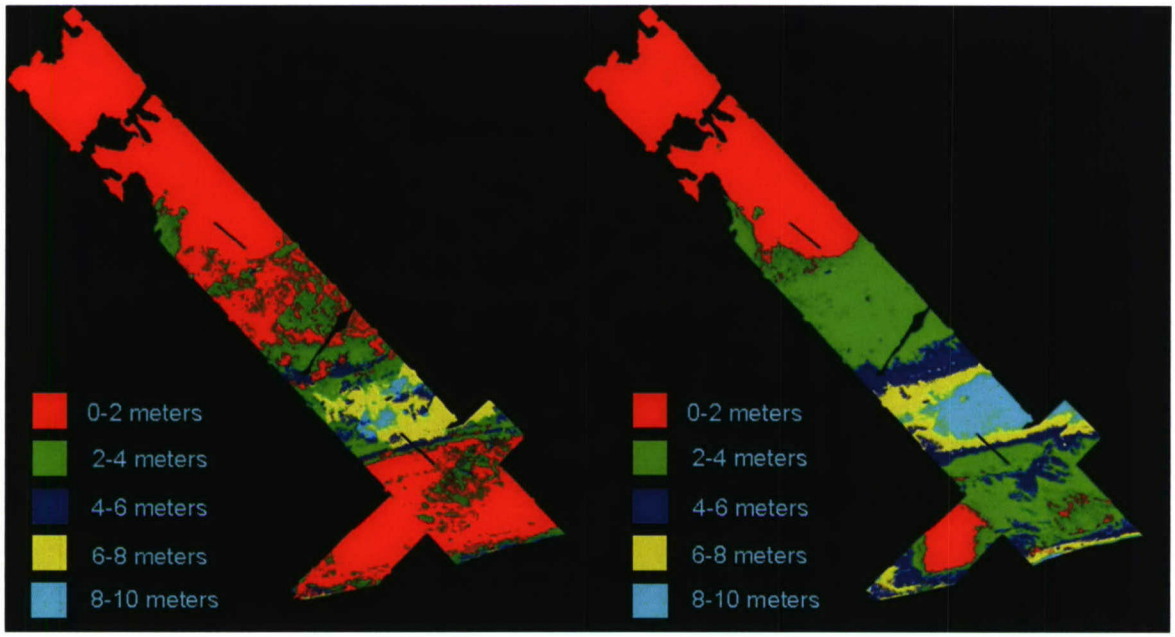


***Figure 14. (LEFT) Absolute difference in depths derived from the old LUT and the SHOALS bathymetry. (RIGHT) Absolute difference in depths derived from the new LUT and the SHOALS bathymetry. Note the increase in bathymetric errors between the old 12K v. the new 200K LUT.***

To investigate the source of misclassification, we selected two pixels from the areas show in Figure 15, and plotted them with the spectrums that were selected from the old and the new LUT (Figure 16 and 17). For the first pixel, the SHOALS derived depth is 14.6 m, the new LUT spectrum selected has a depth of 5.25 m and the old spectrum has a depth of 7 m (Figure 16). The second pixel has the SHOALS derived depth of 7.16 m, the new LUT derived depth of 4.5 m, and the old LUT derived depth of 6.5 m (Figure 17). It was clear that while the database spectrum was better matched to the image spectrum, the retrieve bathymetry was in greater error. Looking further at the spectra in plot 1 of Figure 15, we sought to analyze was how well all the database spectrum with the depth of 14.6 meters fitted the image spectrum. Figure 18 has the image spectrum plotted with all the LUT spectrums with depth of 14.6 meters (Plot 1 of Figure 15).


*Figure 15. Location of Rrs spectra for further analysis of 12K v. 200K LUT differences.*

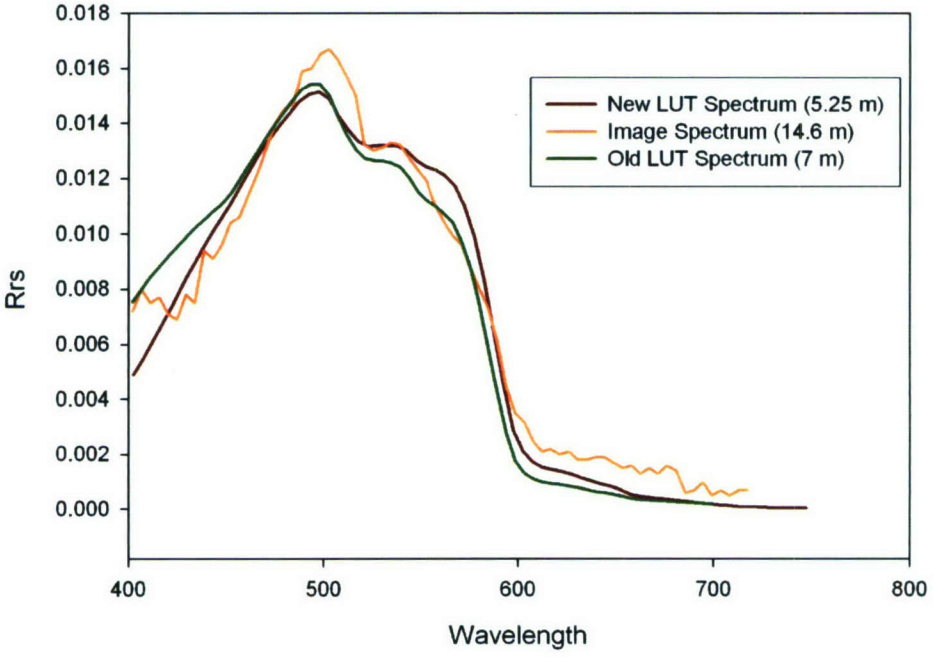


*Figure 16. Image spectrum and the selected LUT spectrums from plot position 1 in Figure 15. Note that the new LUT spectrum matches the Rrs spectra better than the old LUT. However, the new LUT has a greater bathymetric error.*

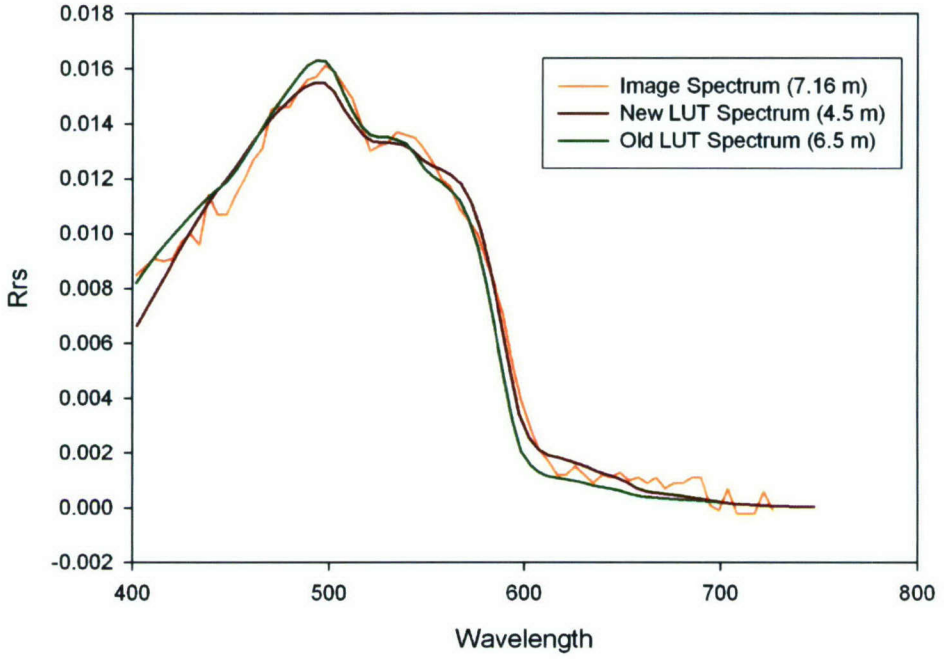


***Figure 17. Image spectrum and the selected LUT spectrums from plot position 1 in Figure 15. Note the note that the new LUT spectrum matches the Rrs spectra better than the old LUT. However, the new LUT has a greater bathymetric error.***

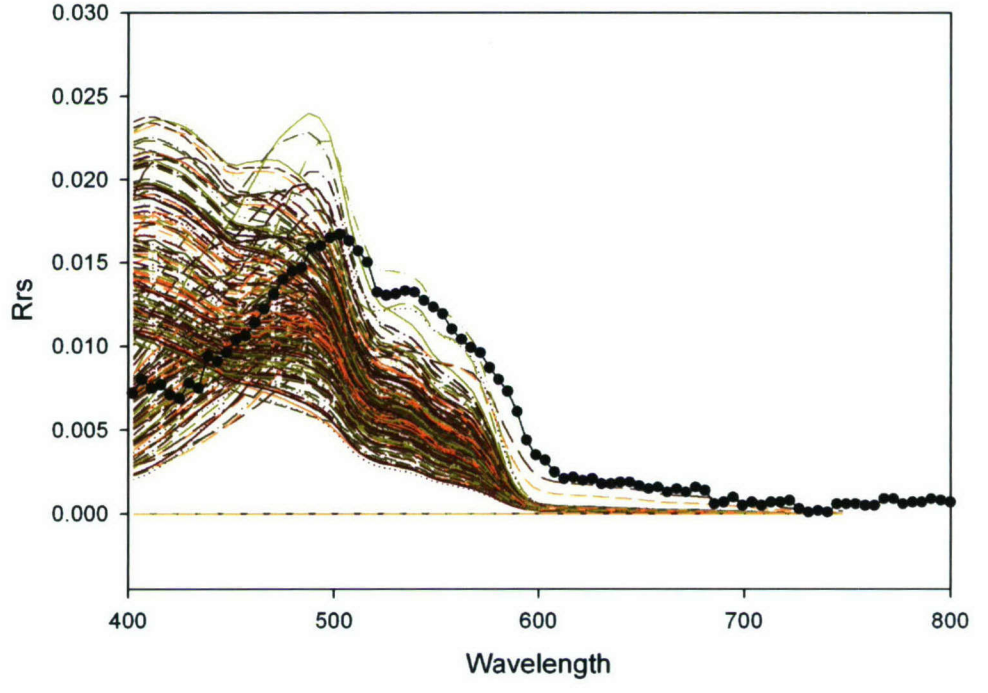

**Figure 18. The image Rrs spectrum from plot 1 in Figure 15 (black line) is plotted with all the 14.6 meter LUT spectrums. Thresholding was done to minimize the number of spectrum in plot to maintain readability.**

Two things are evident from these graphs. The first is that it is possible that the larger database may actually produce greater errors through noise in the Rrs spectrum (Figure 16 and 17), resulting from either sensor or environmental noise components. The second thing evident is that while the depth discretization may produce a finer resolution in the vertical resolution, if the IOPs or the bottom reflectance actually found in the image space are not represented in the LUT database, the depth errors may still be significant (Figure 18).

These results are leading us to develop new methodologies in searching the LUT database, as well as the establishment of confidence indicators to better determine the suitability of a spectrum match. This will be the focus of the FY 2006 projects.

**OBJECTIVES - 2006**

The work for the Look-Up-Table (LUT) approach to inverting remote sensing ended on this grant at the beginning of the year. It continues under a new grant, N000140610370, and again led by PI C. Mobley, N0001406C0177. This grant (N000140110201) was expanded during 2006 to include MultiSpectral Imaging/HyperSpectral Imaging (MSI/HSI) overflights for the Naval Research Laboratory-Stennis Space Center (NRL-SSC) during April 2006. It was also expanded to allow for the purchase of capital equipment to refine the HSI sensor calibration to provide a more robust data stream for the LUT inversion approach.

**APPROACH -2006**

Expansion 1.. Our programs on automated feature extraction from remotely sensed imagery in the coastal zone has been focused on off-shore coastal waters or tidally-driven estuaries with salinities approaching those of off-shore waters. However, there are coastal regions where fresh water inputs into the near-shore environment are significant, dramatically altering the expected IOPs and bottom types within these environments. This will significantly alter the expected error budgets for any bathymetry, bottom classification, target identification, or IOP algorithms designed for saline marine conditions. In addition, the area of operations for Naval Special Boat Teams does not stop at the shoreline; rather the SBTs move inland along river routes to target areas. SBTs have similar bathymetric and shoreline mapping requirements as those operators moving onto traditional beach zone environments. We currently do not have HyperSpectral Imagery (HSI) data for these inshore, fresh water, environments with which to develop, test, and validate our LUT methodology. This expansion proposal is to collect the HSI data stream to continue the development of LUT for ship to shore operations.

This 2006 expansion is to build upon other HSI and LUT efforts by FERI, and the Naval Research Laboratory at Stennis Space Center (NRL-SSC). This collaboration offers the ability to collect the HSI and provide the requisite ground control data at a much less expensive cost point than were we to focus on this collection as a stand alone effort. This collaborative effort will be in the region of the Pearl River, with FERI supplying flight support services, and ortho-rectified airborne HSI and high resolution MultiSpectral Imagery (MSI). NRL-SSC (PI-A. Weidemann) will be responsible for ground support operations, as well as ground control and validation data streams.

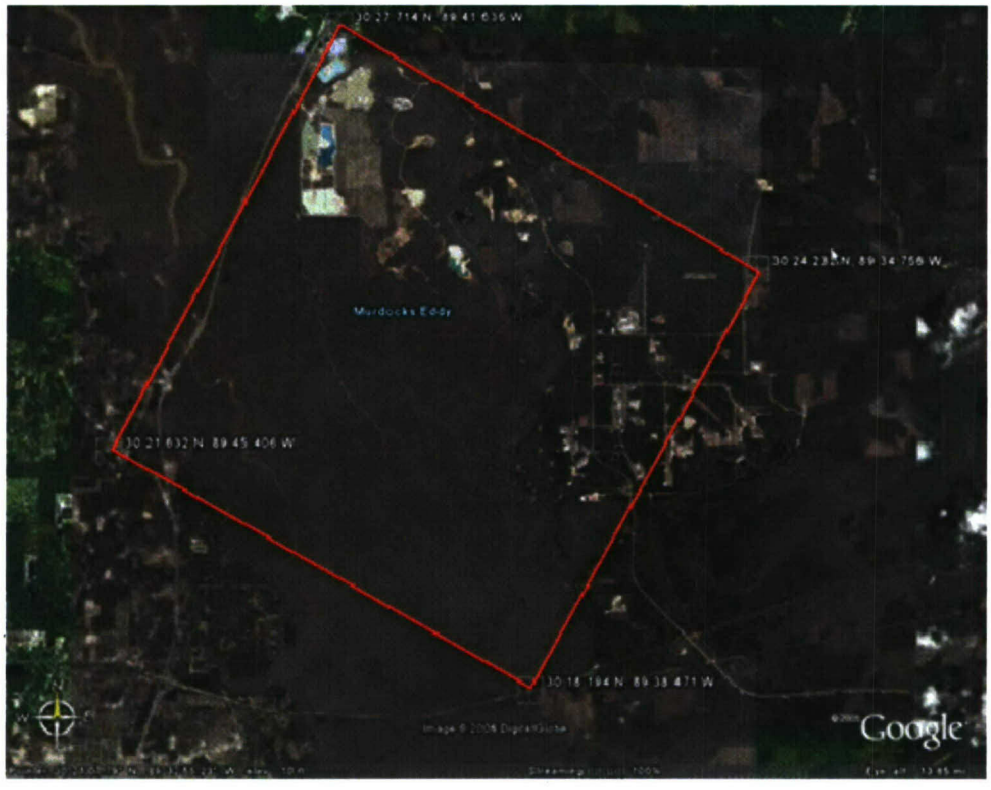


***Figure 19. The region of the Pearl River to be covered by 1 m HSI and 0.15 m MSI between March 31 and April 7, 2006.***

Expansion 2. The overall goal of this LUT project is to develop near-real time processing and algorithms to characterize Very Shallow Water (VSW) BattleSpace Environments (BSE), as well as target detection capabilities for Mine Counter Measures (MCM) using HyperSpectral Imaging (HSI) techniques. This LUT project is focused on the processing and mathematics associated with the development of new quantitative methods to identify targets, classify unknown materials, determine bathymetry, and assess the vertical structure of inherent optical properties in the water. (The HSI data used in this project is, or has been, collected via other funded efforts.) The ability to accomplish these tasks with high confidence and low false-alarm rates is directly dependent on the data quality and error chain associated with the data's collection and processing. This expansion proposal is to develop the capabilities to reduce the uncertainties associated with the beginning steps of the data processing chain.

In order to develop confidence levels and target error rates in our techniques, it is necessary to understand the basic premise of our approach. The LUT methodology is built upon radiative transfer theory and models. The target signal is modeled based on previously measured (in the case of defined targets such as sand or rock) or modeled (in the case of vertically structured absorption and scattering) and compared against the aircraft or satellite measured HSI data, after it has been calibrated and adjusted for illumination and atmospheric effects. The target radiances are traditionally very low compared to the total sensor measured radiance, as the atmospheric signal is frequently greater than 90% of the total measured upwelling radiance. Therefore, any errors and noise associated with the originating HSI sensor data has a magnified effect on the comparison of the atmospherically-adjusted HSI spectra and the modeled target reflectance spectra.

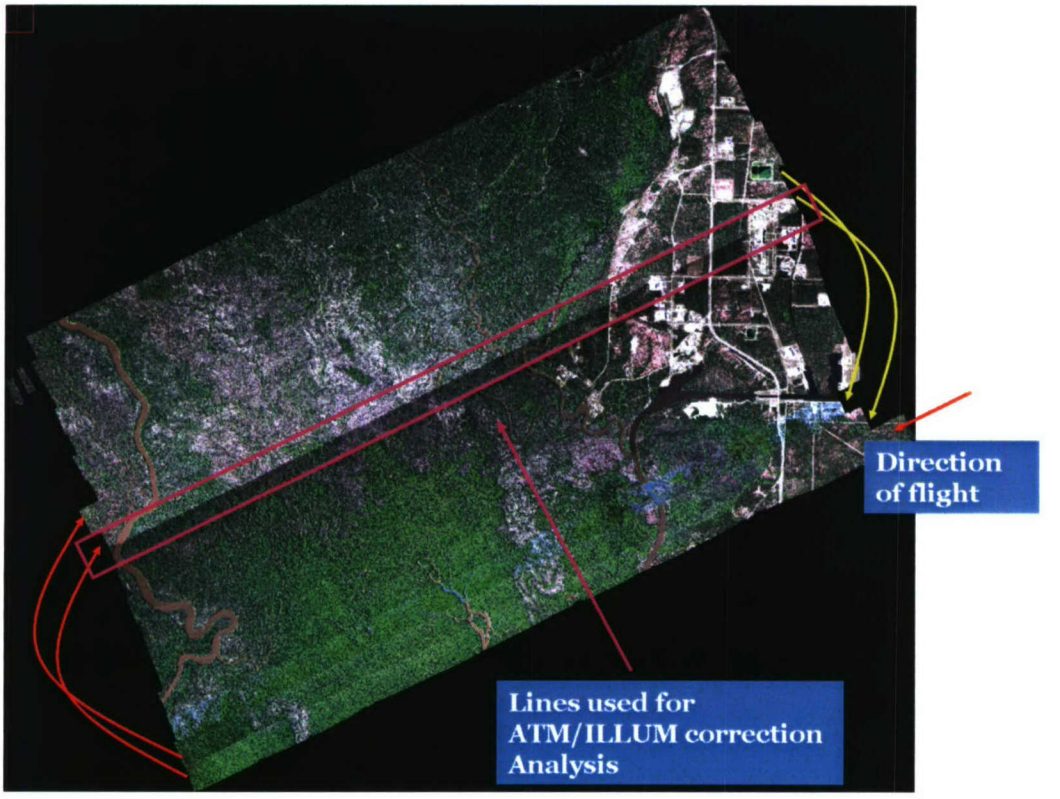


***Figure 20. The region of the Pearl River covered by 1 m HSI and 0.15 m MSI on April 4, 2006. The lines were flow in the afternoon in an ascending race track starting at the southeast corner. The illumination changes are caused by the change in solar elevation during the flight window. The two center lines in the magenta box in the center of the image were the 2nd and 19th flight lines collected, representing beginning and ending of the flight window. These two lines are shown together in Figure 22 after atmospheric and illumination correction.***

There are three broad sources of systematic and unsystematic errors in this methodology. The first is in the error and noise associated with the modeling of the target signals. The second is with the error and noise associated with the calibration of the sensor. The third source is found within the modeling and correction of the illumination and atmospheric conditions. This expansion is focused on reducing the uncertainties associated with the sensor calibration by explicitly measuring the spectral response function of our SAMSON HSI system.

Our current calibration takes into consideration the spectral response function implicitly through the radiometric calibration of multiple color filtered measurements of a diffuse light source (Kohler et al., 2004). While our approach has been reasonably successful at calibrating this type of system, this LUT project calls for the development of the techniques, as well as the explicit calculation of error rates and confidence levels. In order to better achieve these goals, we sought to purchase an Optronic OL 750-M-DS double monochromator. This expansion will allow us to design and conduct more detailed spectral calibrations of our HSI sensor, which in turn will create a more robust HSI data stream reducing the systematic errors in our current processing chain, as well as more completely describe the noise component of the measured spectra. The net result of this expansion will yield better LUT target and classification retrievals, and higher, more definable, confidence in those retrievals.

***Figure 21. Simulated "Man-Down" mission capturing the entire Pearl River from the mouth of the river to the area north of NRL-SSC. The goal was to demonstrate rapid response in airborne HSI collection.***

**WORK COMPLETED - 2006**

Expansion 1. The NRL-SSC Pearl River mission was conducted during the period March 31 – April 6, 2006. We were able to accomplish both the proposed primary mission (Figure 20) on April 4, 2006, as well as a spontaneous secondary mission defined by A. Weidemann to simulate a "man-down" scenario (Figure 21). The primary mission data have been atmospherically-corrected using a technique

devised for missions without ground support (Figure 22), which rendered a full scene mosaic of HSI data (Figure 23).

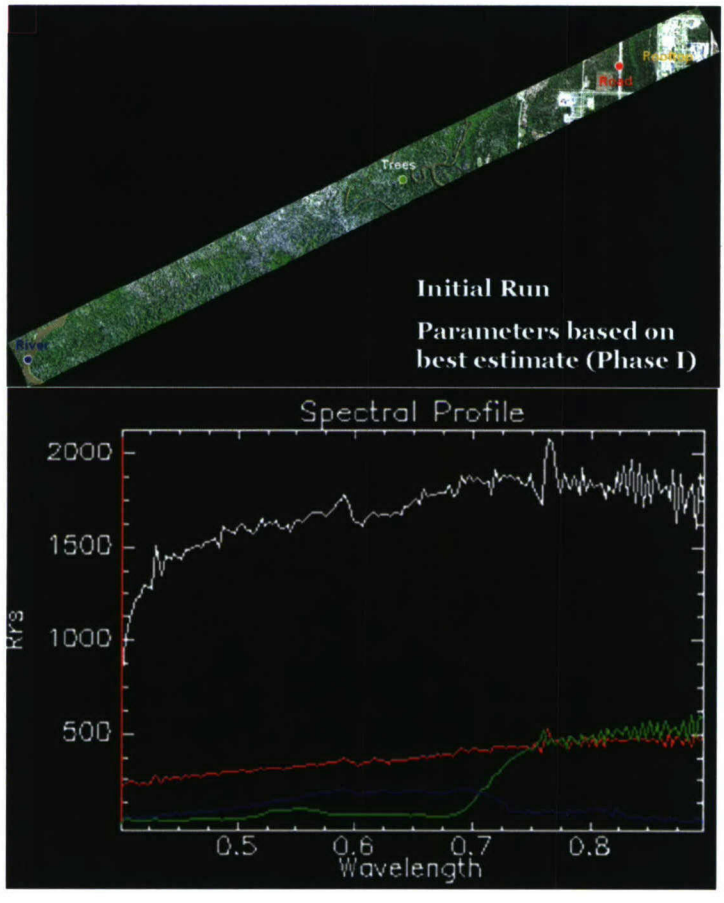


***Figure 22. The flight data represented by the strip at the top of this figure is the combined two center flight lines in the magenta box seen in Figure 2 after atmospheric and illumination correction. The spectra in the bottom of the figure are the points in the top labeled as River (blue point/line), Trees (green point/line), Road (red point/line), and Roof Top (yellow point/white line). Rrs is in units 1/sr * 1000.***

Expansion 2. The double monochromator was delivered in July 2006 (Figure 24) and used to calibrate our 1 m integrating sphere (Figure 24). This calibrated sphere was used to post-mission calibrate our SAMSON HSI sensor from the March and April flight operations. We are working through the differences between the pre-mission calibration data collected at NRL-DC and the post-mission calibration data collected at FERI (Figure 25).

## RESULTS

Expansion 1. Figures 22 and 23 demonstrate one of multiple techniques we have developed to accomplish the atmospheric and illumination correction in near-real time. The method shown in these figures was based on a collection of best estimates of various atmospheric parameters, i.e. water vapor, ozone, aerosol type, during the flight, which allows us to rapidly generate spectral reflectance in a few hours from the end of collection. The man-down mission in Figure 21 demonstrated the ability of our

flight planning, deployment, and processing systems to rapidly respond to a simulated high priority mission.

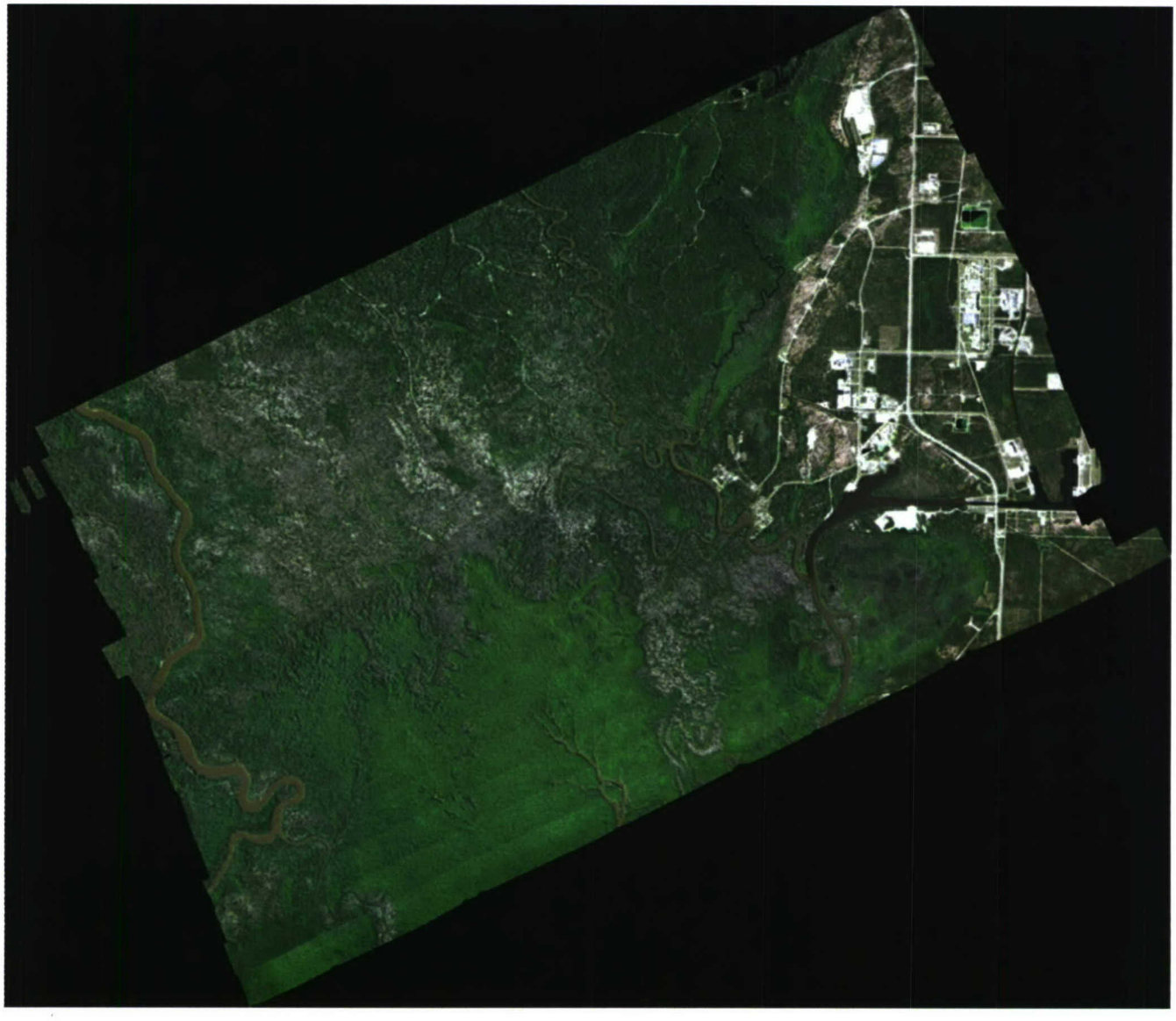

**Figure 23. Environmentally corrected HSI image from data seen in Figure 21.**

Expansion 2. The spectral radiometric calibration of FERI's Labsphere 1 m integrating sphere shows some differences in the calibrated spectral radiant intensity at the 10 lamp illumination setting. This could be caused by a number of factors, including the difference in aging of the bulbs and sphere coating between the NRL's and FERI's spheres. In addition, we expect that there should be some significant differences in the blue because of the use of a single monochromator (versus a double monochromator) in the calibration of the NRL sphere.

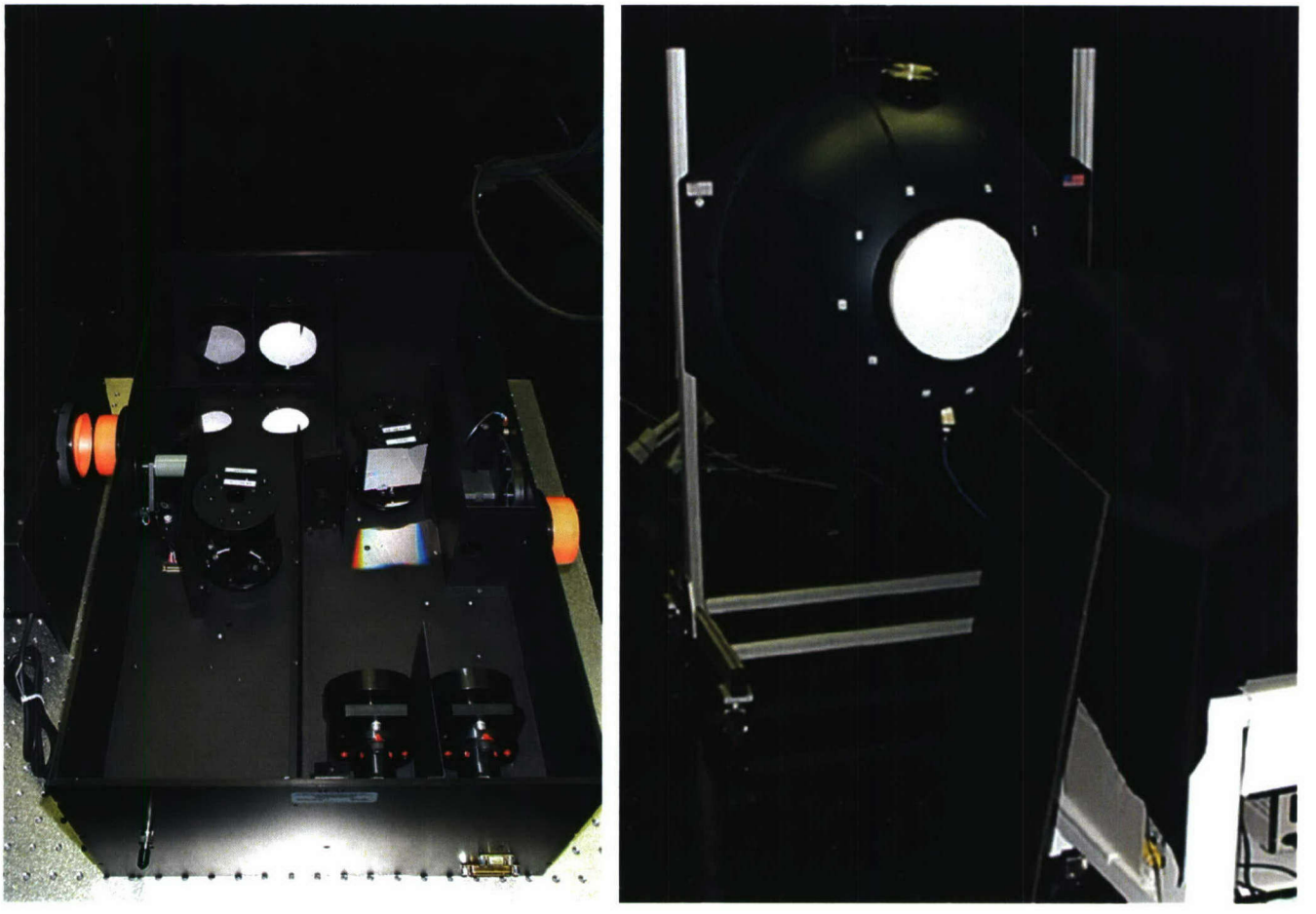

*Figure 24. The Optronic's 750 DM/S Double Monochromator (left) and its use in calibrating FERI's Lapsphere 1 m integrating sphere (right). The double monochromator is covered in a black drop cloth when placed in front of the sphere.*

## IMPACT/APPLICATIONS

Full utilization of the hyperspectral data field from aircraft and satellite data streams will provide the mechanism to invert $R_{rs}$ to depth-dependent optical properties such as absorption, scattering, and bathymetry. These are critical data streams for performance prediction modeling, as well as initialization and validation of predictive optical simulations. This program will provide the tools necessary to rapidly invert $R_{rs}$ data to depth-dependent optical properties.

## IMPACT/APPLICATION – 2006 Expansion

The problem of extracting environmental information from remotely sensed ocean color spectra is fundamental to a wide range of basic and applied science problems. Extraction of bathymetry and bottom classification is especially valuable for planning military operations in denied access areas. No single inversion technique can be expected to be superior in all situations; therefore all techniques must be evaluated. In addition to investigating a new type of inversion, part of our work is to evaluate when the LUT technique is superior to other techniques, and when it is not. This work thus adds to the existing suite of remote sensing analysis techniques. These expansion missions focused specifically on

the ability to reduce the errors in the LUT techniques through better sensor calibration, and on the collection of operational areas of interest for Naval Special Boat Teams.

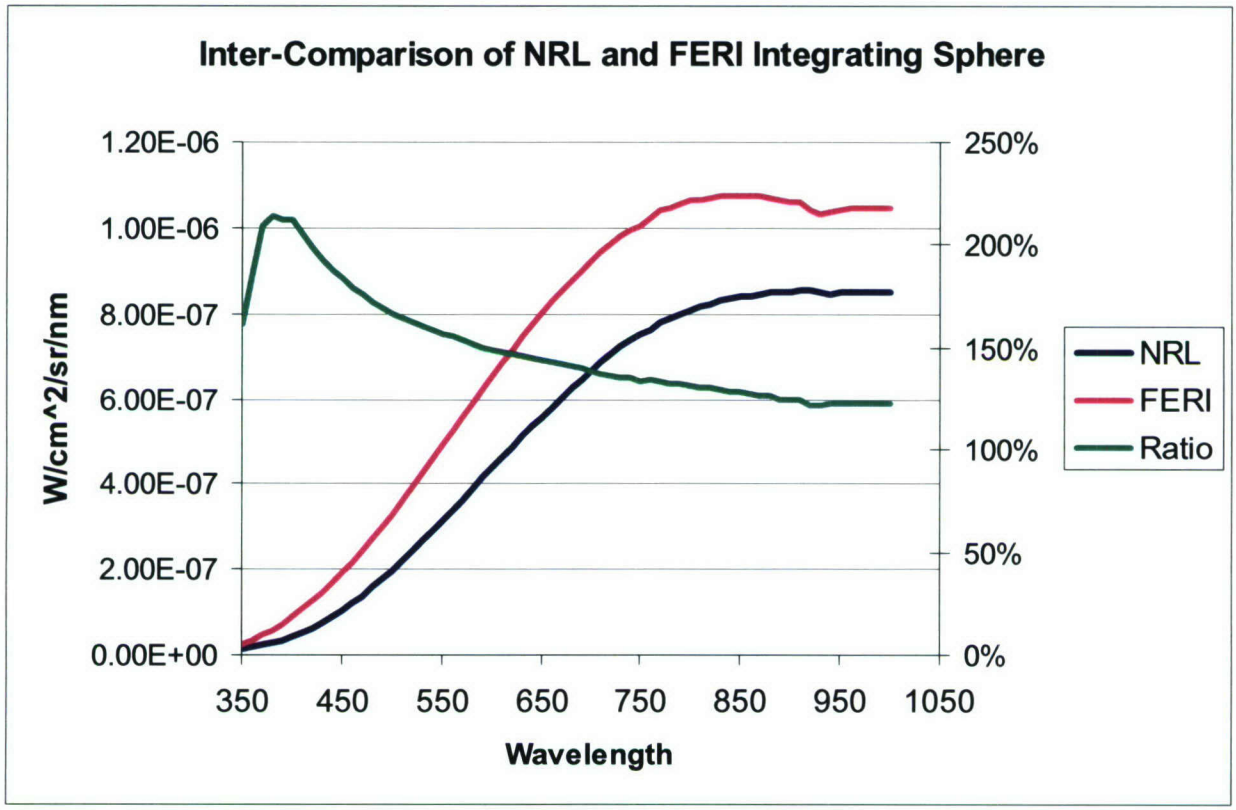


***Figure 25. Inter-comparison of NRL and FERI Integrating Spheres. The ratio is FERI's Sphere at 10 Lamps: NRL's Sphere at 10 Lamps. FERI sphere is brighter, and "bluer" than the NRL sphere. Some of this may be due to the age of the lamps and sphere coating at NRL, as well as the use of a single monochromator in the calibration of the NRL sphere.***

## TRANSITIONS

Various databases of water IOPs, bottom reflectances, and the corresponding $R_{rs}$ spectra, along with the specialized Hydrolight code and spectrum-matching algorithms have been transitioned to the Naval Research Laboratory (Remote Sensing Division) for processing PHILLS and PHILLS-2 imagery.

## RELATED PROJECTS

The work is part of a larger proposal being led by C. Mobley of Sequoia Scientific, Inc. (N0001400D01610001), in coordination with the hyperspectral remote sensing program of C. Davis, Code 7212, Naval Research Laboratory.

## REFERENCES

Guenther, G.C., 2001. Chapter 8. Airborne LIDAR Bathymetry. In: D.F. Maune (Editor), Digital Elevation Model Technologies and Applications: The Dem Users Manual. ASPRS, Washington, DC, pp. 1-69.

Kohler, D.D.R., 2001. An evaluation of a derivative based hyperspectral bathymetric algorithm. Dissertation Thesis, Cornell University, Ithaca, NY, 113 pp.

Lee, Z., Carder, K.L., Mobley, C.D., Steward, R.G. and Patch, J.S., 1999. Hyperspectral remote sensing for shallow waters: 2. Deriving bottom depths and water properties by optimization. Applied Optics, 38(18): 3831-3843.

Lyzenga, D.R., 1978. Passive Remote Sensing Techniques For Mapping Water Depth and Bottom Features. Applied Optics, 17(3): 379-383.

Mobley, C.D., 1994. Light and Water. Academic Press, San Diego, CA, 592 pp.

Mobley, C.D., Sundman, L., Davis, C.O., Montes, M. and Bissett, W.P., 2002. A look-up-table approach to inverting remotely sensed ocean color data, Ocean Optics XVI. Office of Naval Research Ocean, Atmosphere, and Space S&T Department, Santa Fe, NM.

O'Reilly, J.E., Maritorena, S., Mitchell, B.G., Siegel, D.A., Carder, K.L., Garver, S.A., Kahru, M. and McClain, C., 1998. Ocean color chlorophyll algorithms for SeaWiFS. Journal of Geophysical Research, 103(C11): 24,937-24,953.

Philpot, W.P., 1989. Bathymetric mapping with passive multispectral imagery. Applied Optics, 28(8): 1569-1578.

**PUBLICATIONS**

Bissett, W. P., Arnone, R., DeBra, S., Dye, D., Kirkpatrick, G., Mobley, C., and Schofield, O.M. (2005). The Integration Of Ocean Color Remote Sensing With Coastal Nowcast/Forecast Simulations Of Harmful Algal Blooms (HABs). UNESCO Monographs on Oceanographic Methodology- Manual on Harmful Marine Microalgae, UNESCO [submitted, refereed].

Mobley, C. D., L. K. Sundman, C. O. Davis, T. V. Downes, R. A. Leathers, M. J. Montes, J. H. Bowles, W. P. Bissett, D. D. R. Kohler, R. P. Reid, E. M. Louchard, and A. Gleason, 2005. Interpretation of hyperspectral remote-sensing imagery via spectrum matching and look-up tables. *Applied Optics* **44**(17), 3576-3592. [published, refereed]

Schofield, O., Bosch, J., Glenn, S., Kirkpatrick, G., Kerfoot, J., Moline, M., Oliver, M., and Bissett, P. (2005). Harmful Algal Blooms in a Dynamic Environment: How Can Optics Help The Field-Going and Sample-Poor Biologist? UNESCO Monographs on Oceanographic Methodology- Manual on Harmful Marine Microalgae, UNESCO [submitted, refereed].

Bissett, W.P., Arnone, R., DeBra, S., Deterlie, D., Dye, D., Kirkpatrick, G., Schofield, O. and Walsh, J. (2005). Predicting the Inherent Optical Properties and Colored Dissolved Organic Matter Dynamics on the West Florida Shelf. Marine Chemistry, 95, 199-233, [published, refereed].

Glenn, S., Arnone, R., Bergman, T., Bissett, P., Crowley, M., Cullen, J., Gryzmski, J., Haidvogel, D., Kohut, J., Moline, M., Oliver, M., Orrico, C., Sherrell, R., Song, T., Weidemann, A., Chant, R. and Schofield, O., 2004. The Biogeochemical Impact of Summertime Coastal Upwelling on the New Jersey Shelf. Journal of Geophysical Research: 109 (C12S04), [published, refereed].

Chen, R.F., Bissett, W.P., Coble, P., Conmy, R., G. Gardner, B., Moran, M.A., Wang, X., Wells, M.L., Whelan, P. and Zepp, R.G. (2004). Chromophoric Dissolved Organic Matter (CDOM) Source Characterization in the Louisiana Bight. Marine Chemistry, 89(1-4): 257-272, [published, refereed].

Kohler, D.D.R., Bissett, W.P., Steward, R.G. and Davis, C.O., 2004. A New Approach for the Radiometric Calibration of Spectral Imaging Systems. Optics Express, 12(11), [published, refereed].

Mobley, C.D., Stramski, D., Bissett, W.P. and Boss, E., 2004. Optical modeling of ocean waters: Is the Case 1 - Case 2 classification still useful? Oceanography, 17(2): 60-67, [published, refereed].

Oliver, M.J., Kohut, J.T., Irwin, A.J.G., Schofield, O.M., Glenn, S., Moline, M.A., and Bissett, W.P. (2004). Bioinformatic Approaches for Objective Detection of Water Masses. Journal of Geophysical Research, 109(C7): 12, [published, refereed].

Philpot, W.D., Davis, C.O., Bissett, W.P., Mobley, C., Kohler, D.D.R., Lee, Z.P., Snyder, W., Steward, R.G., Gould, R. and Arnone, R., 2004. Bottom characterization from hyperspectral image data. Oceanography, 17(2): 76-85, [published, refereed].

Schofield, O., Arnone, R., Bissett, P., Dickey, T., Davis, C., Finkel, Z., Oliver, M. and Moline, M., 2004. Watercolors in the coastal zone: what can we see? Oceanography, 17(2): 24-31, [published, refereed].

Schofield, O., Bergmann, T., Oliver, M., Moline, M., and Bissett, P. (2004). Inversion of the Bulk Absorption in the Mid-Atlantic Bight and its Utility for Water Mass Analysis in Optically Complex Coastal Waters. Journal of Geophysical Research, 190(C12S04): 12 [published, refereed].

**HONORS/AWARDS/PRIZES**

2004 Small Business of the Year, Finalist, Florida Environmental Research Institute, W. Paul Bissett, Ph.D., Executive Director, Greater Tampa Chamber of Commerce.